A Staggered Time Integration Technique for Spectral Methods

Tian Xiao* and Qing Huo Liu
Electrical and Computer Engineering
Duke University
Durham, North Carolina 27708

1 INTRODUCTION

Spectral methods on unstructured grids developed in recent years provide a general, practical, accurate and efficient tool to model large-scale broadband electromagnetic problems with complex geometry because of their versatility and flexibility, numerical stability and spectral convergence. These new methods introduce a penalty term which is dependent of the jump of fields across the interfaces of the elements to impose the boundary conditions weakly rather than strongly as is classically done. This elegantly splits the differential operator and boundary conditions, thus removing many problems associated with the analysis of stable and accurate pseudospectral approximations.

In this paper, a staggered time integration technique is developed for the spectral methods to make them more efficient in computational time and memory. A method similar to predictor and corrector methods is used in the staggered integration technique to overcome the difficulty of the staggering of the boundary penalty term which is a key ingredient introduced in the spectral penalty methods. Case studies validate the spectral methods and the staggered time integration technique. Practical applications confirm the efficacy of the staggered spectral methods to solve realistic problems in industry and engineering.

2 Formulation

To construct a spectral method on a general unstructured grid, the computational domain is discretized into a number of tetrahedra. By polynomial collocation methods, the unknown fields $\mathbf{E}$ and $\mathbf{H}$ in each tetrahedron of the unstructured grids is assumed to be well approximated as

$$\mathbf{E}(\mathbf{x},t) \approx \sum_{j=0}^{N} \mathbf{E}_j(t) L_j(\mathbf{x}),\ \mathbf{H}(\mathbf{x},t) \approx \sum_{j=0}^{N} \mathbf{H}_j(t) L_j(\mathbf{x}), \tag{1}$$

where $\mathbf{E}_j(t) = \mathbf{E}(\mathbf{x}_j,t)$, $\mathbf{H}_j(t) = \mathbf{H}(\mathbf{x}_j,t)$, and $L_j(\mathbf{x})$ is the 3D multivariate Lagrange interpolation polynomial of order n associated with nodal points $\{\mathbf{x}_j\}$ whose total number is given by $N = \frac{1}{6}(n+1)(n+2)(n+3)$ to allow the polynomial basis to be complete.

The time integration of discretized Maxwell's equations is performed element by element in the spectral method. Thus, the numerical field values across the interface of any two adjacent tetrahedral elements may not be consistent with the correct boundary conditions. To ensure the correct boundary conditions, the change of the flux responding to the jump is obtained by Rankine-Hugonoit jump conditions to satisfy the following relations [4]

$$\hat{\mathbf{n}} \cdot [\mathbf{F}] = \begin{cases} (Z^+ + Z^-)^{-1} \hat{\mathbf{n}} \times (Z^+ [\mathbf{H}] - \hat{n} \times [\mathbf{E}]) \\ (Y^+ + Y^-)^{-1} \hat{\mathbf{n}} \times (-Y^+ [\mathbf{E}] - \hat{n} \times [\mathbf{H}]) \end{cases}, \tag{2}$$

where $[\mathbf{E}] = \mathbf{E}^+ - \mathbf{E}^-$ and $[\mathbf{H}] = \mathbf{H}^+ - \mathbf{H}^-$ measure the jumps in the field values across the interface, and superscripts '+' and '−' refer to the values from neighbor and local elements,

0-7803-7846-6/03/$17.00 ©2003 IEEE

respectively. Here Z denotes impedance and Y denotes conductance. Eq. (2) will act as the penalizing boundary term in the following element-wise formulation for the electric fields

$$\frac{d\mathbf{E}}{dt} = (\mathrm{M}^{\epsilon})^{-1}\,\mathbf{V}\times\mathbf{H} + (\mathrm{M}^{\epsilon})^{-1}\,\mathrm{M}(\sigma\mathbf{E}+\mathbf{J}) + (\mathrm{M}^{\epsilon})^{-1}\,\mathrm{F}\left(\hat{\mathbf{n}}\times\frac{Z^{+}[\mathbf{H}]-\hat{\mathbf{n}}\times[\mathbf{E}]}{Z^{+}+Z^{-}}\right)\Big|_{\delta\mathbf{D}}, \quad (3)$$

and likewise for the magnetic field

$$\frac{d\mathbf{H}}{dt} = (\mathrm{M}^{\mu})^{-1}\,\mathbf{V}\times\mathbf{E} - (\mathrm{M}^{\mu})^{-1}\,\mathrm{F}\left(\hat{\mathbf{n}}\times\frac{Y^{+}[\mathbf{E}]+\hat{\mathbf{n}}\times[\mathbf{H}]}{Y^{+}+Y^{-}}\right)\Big|_{\delta\mathbf{D}}, \quad (4)$$

where $M^{\epsilon}_{ij} = (L_i(\mathbf{x}), \epsilon(\mathbf{x})L_j(\mathbf{x}))_{\mathbf{D}}$, $M^{\mu}_{ij} = (L_i(\mathbf{x}), \mu(\mathbf{x})L_j(\mathbf{x}))_{\mathbf{D}}$, $M_{ij} = (L_i(\mathbf{x}), L_j(\mathbf{x}))_{\mathbf{D}}$, $\mathbf{V}_{ij} = (L_i(\mathbf{x}), \nabla L_j(\mathbf{x}))_{\mathbf{D}}$, $F_{ij} = (L_i(\mathbf{x}), L_l(\mathbf{x}))_{\delta\mathbf{D}}$. Eqs.(3)-(4) can be integrated by some time-advancing techniques, such as the Runge-Kutta methods implemented previously. Next, we will construct a staggered time integrator for the spectral method to save computational cost.

To introduce the staggered time discretization, we define electric field $\mathbf{E}$ at integer time steps and magnetic field $\mathbf{H}$ at half time steps. And then central difference approximations are used to advance $\mathbf{E}$ and $\mathbf{H}$. Unfortunately, some information such as $\mathbf{E}$ at half time steps and $\mathbf{H}$ at integer time steps in the right hand of Eqs. (3) and (4) is not available to complete the central difference approximations. We propose the following method to overcome this difficulty.

An intermediate values of $\mathbf{E}$ at half time steps are first estimated using a mixed difference approximations (backward for magnetic-field terms and forward for electric-field terms),

$$\begin{aligned}\mathbf{E}^{n+1/2} = \mathbf{E}^{n} + \frac{\Delta t}{2}\Big[&(\mathrm{M}^{\epsilon})^{-1}\,\mathbf{V}\times\mathbf{H}^{n+1/2} + (\mathrm{M}^{\epsilon})^{-1}\,\mathrm{M}(\sigma\mathbf{E}^{n}+\mathbf{J}^{n+1/2})\\ &+ (\mathrm{M}^{\epsilon})^{-1}\,\mathrm{F}\left(\hat{\mathbf{n}}\times\frac{Z^{+}[\mathbf{H}]^{n+1/2}-\hat{\mathbf{n}}\times[\mathbf{E}]^{n}}{Z^{+}+Z^{-}}\right)\Big|_{\delta\mathbf{D}}\Big]. \end{aligned} \quad (5)$$

where Δt is the time step and the superscripts refer to the temporal indices. After obtaining $\mathbf{E}$ at half time steps the central difference approximation is used to advance electric field $\mathbf{E}$ to the next integer step as

$$\begin{aligned}\mathbf{E}^{n+1} = \mathbf{E}^{n} + \Delta t\Big[&(\mathrm{M}^{\epsilon})^{-1}\,\mathbf{V}\times\mathbf{H}^{n+1/2} + (\mathrm{M}^{\epsilon})^{-1}\,\mathrm{M}(\sigma\mathbf{E}^{n+1/2}+\mathbf{J}^{n+1/2})\\ &+ (\mathrm{M}^{\epsilon})^{-1}\,\mathrm{F}\left(\hat{\mathbf{n}}\times\frac{Z^{+}[\mathbf{H}]^{n+1/2}-\hat{\mathbf{n}}\times[\mathbf{E}]^{n+1/2}}{Z^{+}+Z^{-}}\right)\Big|_{\delta\mathbf{D}}\Big]. \end{aligned} \quad (6)$$

The advance of $\mathbf{H}$ is similar. First the intermediate values of $\mathbf{H}$ at integer time steps are estimated as

$$\begin{aligned}\mathbf{H}^{n+1} = \mathbf{H}^{n+1/2} + \frac{\Delta t}{2}\Big[&(\mathrm{M}^{\mu})^{-1}\,\mathbf{V}\times\mathbf{E}^{n+1}\\ &- (\mathrm{M}^{\mu})^{-1}\,\mathrm{F}\left(\hat{\mathbf{n}}\times\frac{Z^{+}[\mathbf{E}]^{n+1}+\hat{\mathbf{n}}\times[\mathbf{H}]^{n+1/2}}{Y^{+}+Y^{-}}\right)\Big|_{\delta\mathbf{D}}\Big]. \end{aligned} \quad (7)$$

And then using the central difference approximation, the magnetic field $\mathbf{H}$ is advanced as

$$\begin{aligned}\mathbf{H}^{n+3/2} = \mathbf{H}^{n+1/2} + \Delta t\Big[&(\mathrm{M}^{\mu})^{-1}\,\mathbf{V}\times\mathbf{E}^{n+1}\\ &- (\mathrm{M}^{\mu})^{-1}\,\mathrm{F}\left(\hat{\mathbf{n}}\times\frac{Z^{+}[\mathbf{E}]^{n+1}+\hat{\mathbf{n}}\times[\mathbf{H}]^{n+1}}{Y^{+}+Y^{-}}\right)\Big|_{\delta\mathbf{D}}\Big]. \end{aligned} \quad (8)$$

Now we estimate the error bound of the staggered time integrator. Assume the time interval $[a, b]$ is divided into N subintervals of equal length $\Delta t = \frac{b-a}{N}$. The time integrator can be expressed

$$\mathbf{T}_N f = \Delta t[f_a(a + \Delta t/2) + f_a(a + 3\Delta t/2) + \cdots + f_a(b - \Delta t/2)] \tag{9}$$

which approximates the integration $\mathbf{I}f = \int_a^b f(t)dt$ where $f_a(t) = f(t) + O(\Delta t^2)$ is the prediction of $f(t)$. Using Taylor expansion, the error bounds are estimated as

$$|\mathbf{I}f - \mathbf{T}_N f| \leq \Delta t^2 \frac{b-a}{12} M_2 \quad \text{where} \quad \mathrm{M_2} := \max\left\{|\mathrm{f_a''(t) - f''(t)}| : \mathrm{t} \in [\mathrm{a, b}]\right\}. \tag{10}$$

Thus, the staggered time integrator is a 2nd-order scheme. Compared with 2 stage 2nd-order Runge-Kutta methods, it requires about 1/4 less memory and 1/3 less CPU time and is especially suitable for lower-order spectral methods.

3 Numerical Results

First the staggered time integration technique for spectral methods is validated by 5 stage 4th-order Runge-Kutta integration method for the radiation of an electric dipole source located at the center of a cylinder. The cylinder of radius 0.3 m and length 0.6m has a relative permittivity 2 and relative permeability 1. The dipole is polarized along $+z$ direction and has a time-function of the first derivative of Blackman-Harris window function with the central frequency 600 MHz. A 3rd-order spectral method with staggered time integration technique is exploited to model the electromagnetic radiation. The results shown in the left figure in Fig. 1 illustrate that the numerical results agree well with those of the Runge-Kutter integration method. The surface mesh of the cylinder is shown in the right figure in Fig. 1.

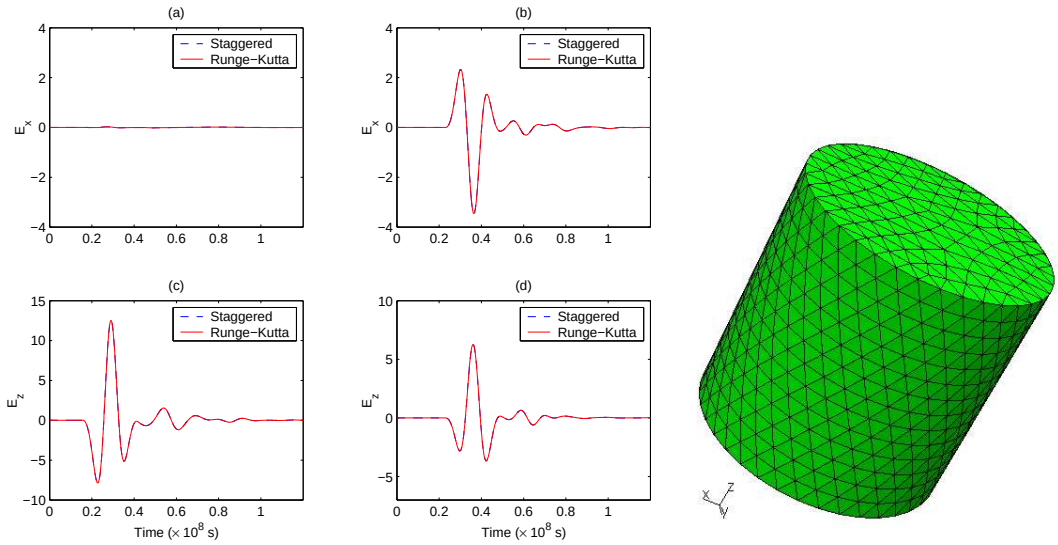

Figure 1: Validation of staggered time integration techniques. (a)(c): E_x and E_z at $(0.35\mathrm{m}, 0.0\mathrm{m}, 0.0\mathrm{m})$; (b)(d): E_x and E_z at $(0.35\mathrm{m}, 0.3\mathrm{m}, 0.3\mathrm{m})$.

The scheme is then applied to model photonic bandgap materials. The scaffold structure with lattice constant of 1.0 μm and dielectric width of 0.125 μm and dielectric constant 13 is modeled. The finite photonic crystal consists of $5 \times 5 \times 5$ periods as in the left panel of Fig. 2. A source is put on the center of one face of the cube and several observation points

are put on the opposite face. Band gap of the photonic crystal is computed as shown in the right panel of Fig. 2 by comparison of the spectrum of the received fields at observation points with that of the source. The bandgap is clearly observed at the normalized frequency band between 0.390–0.425.

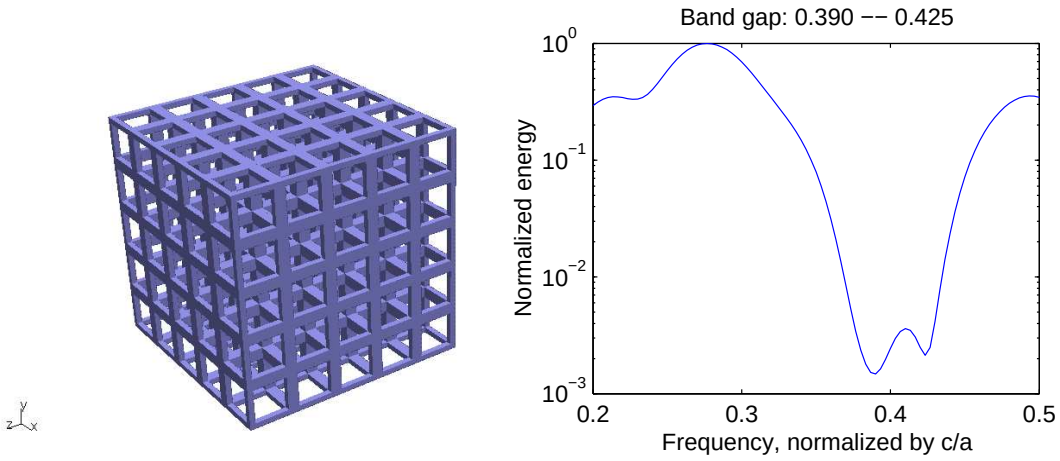

Figure 2: A photonic crystal of scaffold structure and its spectral response.

4 Conclusions

The spectral methods on unstructured grids developed in recent years provide a flexible, accurate and efficient tool to model large-scale broadband electromagnetic problems with complex geometry. In this paper, a staggered-time integrator is introduced in the spectral methods to further improve their computational efficiency. A method similar to predictor and corrector methods are used in the staggered time integration technique to overcome the difficulty of the staggering of the boundary penalty term. Compared with other 2nd-order time integration methods, it requires less memory and CPU time. Thus it is especially suitable for lower-order spectral methods. Case studies of the radiation of a electric dipole source in a cylinder validate the technique. Applications in the modeling of photonic bandgap materials are shown to confirm the efficacy of the method.

References

[1] J. S. Hesthaven, and T. Warburton, "Nodal High-Order Methods on Unstructured Grids I. Time-Domain Solution of Maxwell's Equations," *J. Comput. Phys*, vol.181, pp.186-221, 2002.

[2] J. S. Hesthaven, "From electrostatics to almost optimal nodal sets for polynomial interpolation in a simplex," *SIAM J. Numer. Anal.*, vol.35, pp.655-676, 1998.

[3] Q. H. Liu, "The PSTD algorithm: A time-domain method requiring only two cells per wavelength," *Microwave Opt. Technol. Lett.*, vol. 15, pp.158-165, 1997.

[4] A. H. Mohammadian, V. Shankar, and W. F. Hall, "Computation of electromagnetic scattering and radiation using a time-domain finite-volume discretization procedure," *Comput. Phys. Communications*, vol.68, pp.175-196, 1991.

[5] G.-X. Fan, and Q. H. Liu, "A well-posed PML absorbing boundary condition for lossy media," *IEEE Antennas and Propagat. Soc. Intl. Symp.*, vol. 3, pp. 2-5, Jul. 2001.